Supplementary Information

A dual-switch fluorescence biosensor with entropy-driven and DNA walker cascade amplification circuit for sensitive microRNA detection

Zikang Xie‡,[a] Zhaolong Tang‡,[a] Xindie Zhuang‡,[a] Xinhao Li,[a] Baozheng Wang,[a] Hong Wang*,[a] and Yingwei Zhang*,[a]

a State Key Laboratory of Chemical Resource Engineering, College of Materials Science and Engineering, Beijing University of Chemical Technology, Beijing 100029, China.

1. AuNPs characterization

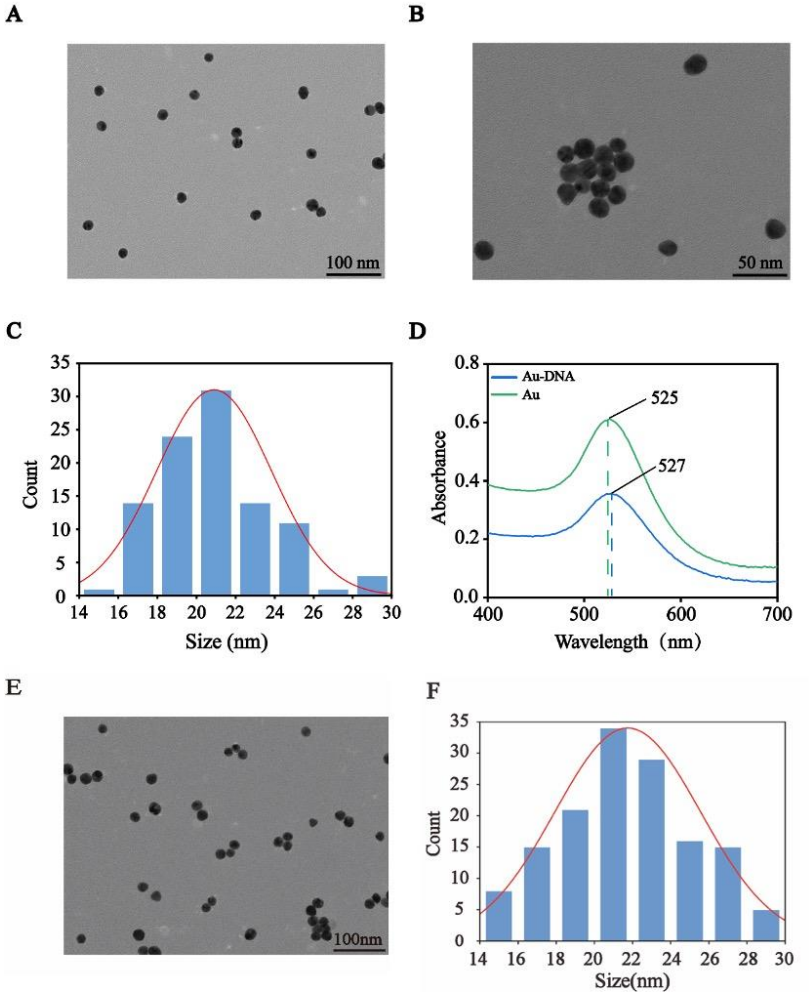

Fig.S1 Characterization of the gold nanoparticles. (A) and (B) TEM images of gold nanoparticles with different magnification (C) Particle size distribution of gold nanoparticles; (D) UV-vis absorption spectrum of gold nanoparticles before and after DNA modification. (E) TEM image of gold nanoparticles after DNA modification; (F) Particle size distribution of gold nanoparticles after DNA modification.

Fig.S1 presents the morphological features of gold nanoparticles prepared using the tannic acid method. Through ImageJ software, a number of gold nanoparticle samples with different magnifications were selected and the distribution statistics of their particle sizes were performed. As shown in Fig.S1 (A), the prepared gold nanoparticles exhibited good dispersion in solution with uniform particle size, showing a typical Gaussian distribution pattern. The average particle

size was measured to be 21 nm. Fig.S1 (D) demonstrates the characteristic peak of gold nanoparticles measured using a UV-Vis spectrophotometer, which was located at around 525 nm. When the surface of the gold nanoparticles was modified with DNA, the position of the characteristic peak was red-shifted and moved to around 527 nm, this phenomenon indicates that the DNA strands have been successfully modified on the surface of the gold nanoparticles. Figure S1(E) and (F) present the TEM image and the particle size distribution of gold nanoparticles after DNA modification. A similar size distribution was observed, confirming that DNA modification does not affect the size and morphology of the AuNPs.

2. Optimization of Walker, Lock, and T Chain Hybridization Ratios

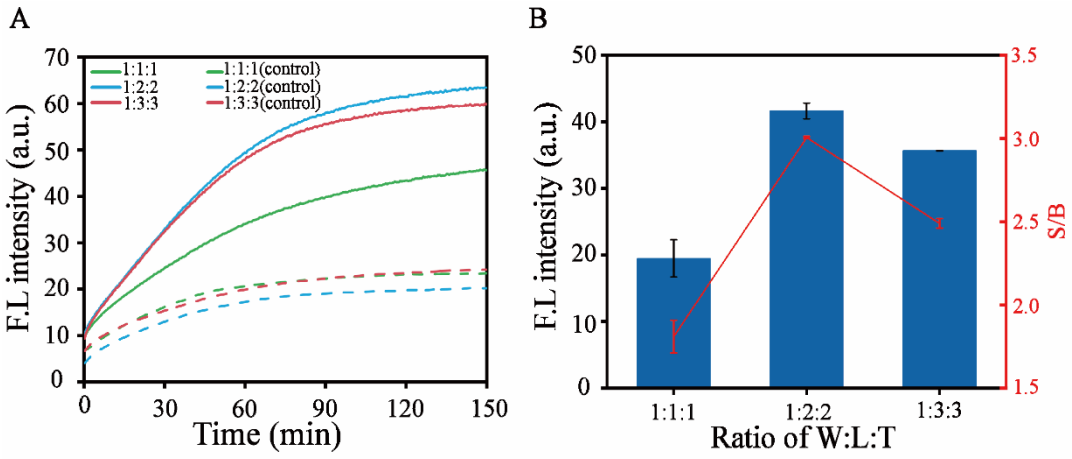

Fig.S2 Optimization of the reaction ratio between walker, lock, and T strands. (A) Real-time fluorescence curves for different ratio groups; (B) Fluorescence net increment and signal-to-background ratio of different proportional groups.

Theoretically, the ideal reaction ratio of walker chains, lock chains, and T chains in the EDC system is 1:1:1. However, to ensure that the walker chains are completely blocked by the

hybridized lock and T strands—preventing any unblocked walker chains from triggering false positive background signals—it is necessary to increase the proportion of lock chains and T chains relative to the walker chains. Any excess lock chains and T chains can be removed in subsequent steps of gold nanoparticle modification by centrifugation, which helps avoid their potential impact on the experimental results. To this end, we explored different hybridization ratios of walker, lock, and T chains for modifying AuNPs, and we compared the fluorescence signals of the experimental group with that of the control group without miRNA21 using RT-qPCR, as shown in Fig S2. When comparing the fluorescence signals of the three different background groups, the 1:2:2 ratio group exhibited the lowest background signal. Additionally, a comprehensive comparison of fluorescence recovery under the three ratios indicated that under the conditions of 1:2:2 and 1:3:3, the net increase in fluorescence intensity due to the cascade reaction was significantly higher. Considering that the 1:2:2 ratio group had a lower signal-to-noise ratio, we selected 1:2:2 as the optimized ratio for subsequent experiments.

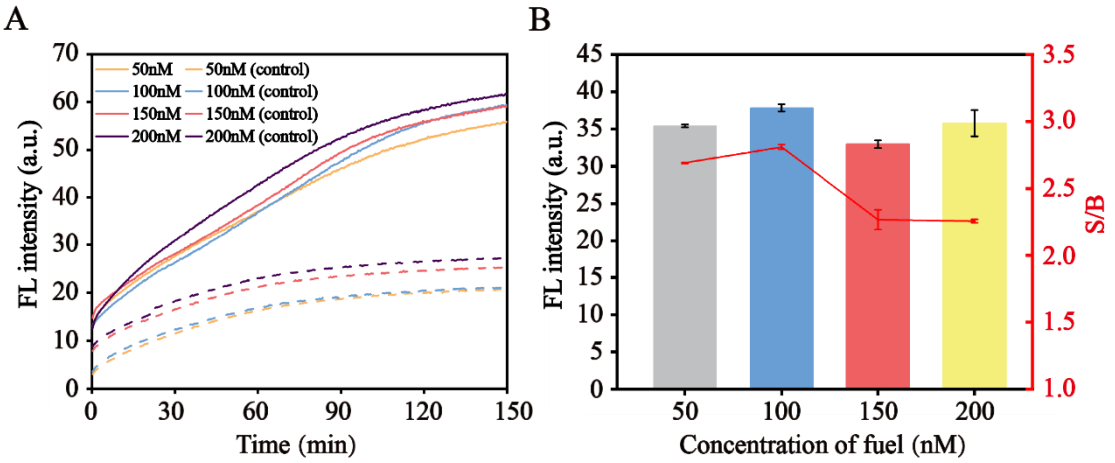

Fig.S3 Optimization experiments for fuel concentration. (A) Real-time curves of fluorescence intensity with different fuel concentrations; (B) Fluorescence net increment and signal-to-background ratio with different concentrations of fuel strand.

3. Optimization of APE1 Enzyme Concentration

APE1 enzyme acts as a driving force for the continuous movement of DNA walkers on the sub-chain, playing a decisive role in the generation of fluorescence signals in the experiment. A concentration of APE1 that is too low may lead to insufficient cleavage at the AP sites on the walker-sub chain, preventing the DNA walker from releasing and moving continuously, which results in a weaker final fluorescence signal. Conversely, an excessively high concentration of APE1 may trigger non-specific cleavage, increasing background signals and introducing unpredictable variables. Therefore, determining an appropriate concentration of APE1 is crucial for the success of the experiment.

The selected enzyme concentrations were 8× APE1 (140 U/mL), 9× APE1 (157 U/mL), 10× APE1 (175 U/mL), 12× APE1 (210 U/mL), 13× APE1 (227.5 U/mL), and 14× APE1 (245 U/mL), while the control group included the corresponding APE1 concentrations without adding the target miRNA. As shown in Fig.S4(A), with the concentration of target miRNA21 fixed at 100 nM, the fluorescence signal of the experimental group significantly increased with the rise in APE1 concentration. At the lower concentration (140 U/mL), the fluorescence signal was insufficient, indicating inadequate cleavage at the AP sites on the sub-chain. When the concentration of APE1 exceeded 175 U/mL (10×), the fluorescence signal increased. However, as the concentration of APE1 continued to rise, the background fluorescence signal in the control group without the target also significantly increased. Particularly, when APE1 concentration was above 210 U/mL (12×), there was a marked increase in background fluorescence. This could be due to the intrinsic 3'-5' exonuclease activity of APE1; when its concentration exceeds a critical value, it may begin cleaving the sub-chain directly from the 3' end, leading to fluorescence signal release.

Further processing and comparison of the experimental and control group data at different enzyme concentrations, as shown in Fig.S4 (B), indicated that the net increase in fluorescence signal gradually increased with rising APE1 concentrations. This suggests that a high concentration of APE1 provides efficient driving force for the walker’s continuous movement on the gold nanoparticle surface sub-chain. However, the signal-to-background ratio (S/B) exhibited a clear peak, with the optimal S/B at an APE1 concentration of 175 U/mL (10×). Considering the net

increase in fluorescence signal, signal-to-background ratio, and the need to minimize background fluorescence in the control group, we ultimately selected 175 U/mL as the optimized concentration of APE1 enzyme for the experiment. This concentration ensures efficient walking of the DNA walker while keeping non-specific cleavage-induced background signals at a lower level.

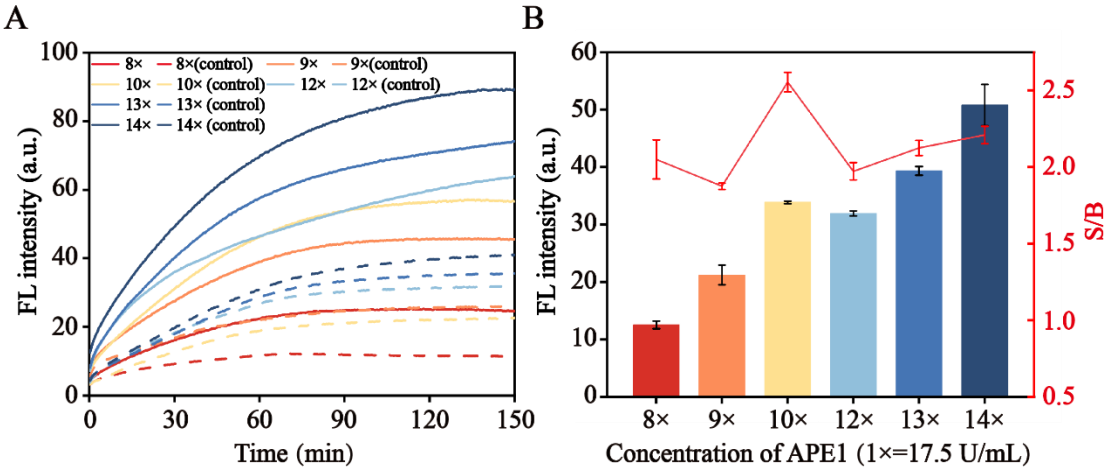

Fig.S4 Fluorescence response to APE1 enzyme with different concentrations. (A) Real-time curves of fluorescence intensity with different APE1 enzyme concentrations; (B) Net fluorescence increases and signal-to-background ratio for different APE1 enzyme concentration groups.

Table S1. The detailed sequence of these oligonucleotides

DNA	Sequence	Length/nt
sub	TTTATGAGGACCGGC**X**CAAGAGAT-FAM	23
Lock	TCAACATCAGTCTGATAAGCTATAGGGCTCACTATTTCGACCGGC	45
T-DNA	CCCTATAGCTTATCAGACT	19
Walker(T30)	TTTTTTTTTTTTTTTTTTTTTTTTTTTTTTATCTCTTGAGCCGGTCGAAATAGTGAG	57
Fuel	GCGGGTCGAAATAGTGAGCCCTATAGCTTATCAGACT	37
miRNA155	UUAAUGCUAAUCGUGAUAGGGGU	23
miRNA21	UAGCUUAUCAGACUGAUGUUGA	22
MDR1 mRNA	CAAGUUAAAGGGGCUAUAGGU	21
Let 7a	UGAGGUAGUAGGUUGUAUAGUU	22

Note: X represents the AP site recognized by APE1, and the leg sequence on the walker strand was underlined.

4. Experimental supplementary section

4.1 Verification of the feasibility of the experiment by real-time fluorescence quantitative

In order to verify the feasibility of the experiment, after the initial validation in polyacrylamide gels, the fluorescence detection technique was further used to monitor the signal changes. Considering that the experimental design involves two key response factors, miRNA21 and APE1 enzyme, the following four sets of controlled experiments were designed to systematically assess their effects:

① Au+fuel

② Au+fuel+miRNA21

③ Au+fuel+APE1

④ Au+fuel+miRNA21+APE1

As described before, walker-lock-T duplex and sub strands were modified onto the surface of AuNPs in a 1:7 ratio. The volume of each sample was fixed to 20 μL, and then the corresponding reactants were added to each PCR tube with 0.5 nM Au, 100 nM fuel, 100 nM miRNA21, and 175 U/mL APE1 enzyme (10×).

RT-qPCR parameter pairs with the same parameters were used to perform each experiment with the following parameter settings: temperature of 37°C, 800 cycles of thermostatic reaction, and an interval of 5 s between each cycle.

4.2 Optimization of experimental parameters by RT-qPCR

After verifying the experimental feasibility with fluorescence detection, the various reaction conditions of the experiment need to be explored in order to achieve the appropriate fluorescence signal and the lowest background signal for the experimental group.

To ensure that the walker chain can be completely enclosed and the walker-lock-T hybridization chain formed is stable enough. The walker strand, lock strand and T strand were mixed in the ratios of 1:1:1, 1:2:2 and 1:3:3, respectively, and then annealed and reacted in PCR, and then the hybridized DNA was modified on top of the AuNPs using the n-butanol method.

For entropy drive fuel chain is the fuel that provides the reaction to continue, and the difference in fuel chain concentration affects the progress of the reaction. However, too much fuel chain can lead to a greater chance of non-specific hybridization with the lock chain, which can produce non-essential background signals. Therefore, an optimization of the concentration of fuel based on the four groups of 50 nM, 100 nM, 150 nM, 200 nM.

APE1 enzyme, as a switch in this experiment, is a critical component for APE1 responsiveness. We explored the appropriate APE1 enzyme concentration and optimized to obtain the best experimental and background group signals based on 5 groups of 8×APE1 enzyme (140 U/mL), 9×APE1 enzyme (157 U/mL), 10×APE1 enzyme (175 U/mL), 13×APE1 enzyme (227.5 U/mL)

and 14×APE1 enzyme (245 U/mL), and calculate the signal-to-noise ratio.

4.3 Detection of different concentration targets by RT-qPCR in real time

We used the above already optimized experimental conditions for different concentrations of miRNA21. The changes in fluorescence intensity brought about by miRNA21 concentrations from 100 nM, 50 nM, 20 nM, 10 nM, 5 nM, 2 nM, 1 nM, 0.2 nM, 0.1 nM, 50 pM, 40 pM, and 0 nM were explored while ensuring that the other conditions were consistent. The limit of detection was calculated according to the standard calculation method LOD = 3 σ /S, where σ is the standard deviation and S is the slope.

4.4 Detection of target selectivity and enzyme selectivity by RT-qPCR in real time

To validate the specificity of the designed biosensor assay, we used other miRNAs associated with oncogenes in tumor cells (miRNA155, let-7a, MDR1 mRNA) instead of miRNA21. the effect of other biomarkers on the fluorescence signal was examined in RT-qPCR. At the same time, it was ensured that the concentration of other miRNA was consistent with the concentration of the detection target.

In order to verify the responsiveness issue of APE1 enzyme, only the species of the added enzyme was changed while ensuring that all other conditions remained unchanged. The enzymes chosen to be added include APE1, UDG, FEN1, λ Exo, blank, and mixture (a mixture of all of the above enzymes), and it was observed in RT-qPCR to see if the other kinds of enzymes would produce an interfering signal to the experiment.

4.5 Culture different kinds of cells

In order to verify the detection effect of the biosensing platform designed in this paper in real cells, experiments need to be conducted in cell lysates. Cells that satisfy both miRNA21 and APE1

enzyme overexpression are selected, along with human normal cells as a control group. The details are as follows: MCF-7 (human breast cancer cells), Hela cells (cervical cancer cells) and HEK-293T cells (human embryonic kidney cells).

MCF-7 cells as a common human breast cancer cells are often used in the experiment, the following MCF-7 cells as an example of cell culture, other cell operation is the same. Step 1, remove MCF-7 cells from the cryopreservation environment and thaw the cells in a water bath. Step 2, centrifuge the culture medium centrifuge tube containing thawed cells, aspirate the upper layer of waste liquid with a pipette gun, and then re-suspend it. Step 3, utilizing a cytotechnology plate to determine the concentration of cells after culturing. Step 4, the counted cells are inoculated at the desired density into Petri dishes containing pre-warmed medium. Step 5, place the inoculated cell culture dish into a 37℃, 5% CO_2 cell culture incubator and continue to culture. Step 6, change the medium every 2-3 days to maintain the growth and healthy state of the cells. Step 7, cell passaging generally requires a cell density of 80-90%, and then the cells are treated with digestive solution such as trypsin, and the cells are re-inoculated into a new culture dish to maintain cell viability and growth status.

4.6 Extraction of cell lysate

The extraction of cell lysate is mainly divided into the following steps: cell culture, cell crushing, configuration of suitable lysate, centrifugation and aspiration of supernatant. The specific operation is as follows: use a cell counting plate to count the number of cells, and then culture the appropriate number of cells in a six-well plate. When the cell apposition density reaches 80%, the next operation can be carried out. The configuration of the cell lysate requires a low-temperature environment to maintain the activity of intracellular proteins. For this purpose, crushed ice can be placed in a foam box to create an ideal low-temperature experimental environment. Prepare intracellular protein extraction lysate and add the lysate to each well in a six-well plate and react for 10 minutes. The lysed cytosol was aspirated into a centrifuge tube and centrifuged in a low temperature centrifuge at 4° C 12000 rpm for 10 minutes. After centrifugation was completed, the supernatant was carefully collected and transferred to a refrigerator for cryopreservation. The centrifuged cell sediment and residue were discarded as waste.

Table S2. A comparison of analytical performances of different strategies for miRNAs detection

Method	Target	Detection range	Linear range	Detection limit	Reference
Fluorescence	miRNA-21	0-100nM	0-10nM	0.5nM	1
Fluorescence	miRNA-125b	0-1000nm	0.5-200nM	0.1nM	2
Fluorescence	miRNA-21	0-200nM	0.5-200nM	0.5nM	3
Visualization detection	miRNA-155	0-300nM	0.05-300nM	50pM	4
Glucose Meter signal	miRNA-21	0-50nM	0-1nM	200pM	5
Fluorescence	miRNA-21	50pM-20nM	50pM-20nM	50pM	6
Fluorescence	miRNA let-7a	0-250nM	1nM-100nM	1nM	7
Fluorescence	miRNA-21	0-100nM	40pM-100nM	40pM	This work

Reference

1. L. Li, Y. Gong, Q. Lin, S. He, C. Xing and C. Lu, *Sens. Actuators B: Chem.*, 2024, **417**, 136046.
2. Y. Gu, R. Bai, X. Qiu, X. Wang, S. Lu, C. M. Li and C. Guo, *Anal. Chem*, 2024, **96**, 7609-7617.
3. S. Yue, X. Xu, L. P. Jiang, H. Yao and J. J. Zhu, *Anal. Chem*, 2025.
4. C. Wang, Y. Zhang, C. Liu, S. Gou, S. Hu and W. Guo, *Biosens. Bioelectron*, 2023, **225**, 115073.
5. Q. Wang, Y. He, S. He, S. Yu, Y. Jiang and F. Wang, *Chem Commun*, 2023, **59**, 1345-1348.
6. T. Yang, J. Fang, Y. Guo, S. Sheng, Q. Pu, L. Zhang, X. Ou, L. Dai and G. Xie, *Microchim. Acta*, 2019, **186**, 574.
7. L. Nie, X. Zeng, L. Hongbo, S. Wang, Z. Lu and R. Yu, *Anal. Chim. Acta* 2023, **1269**, 341392.